Regular hexagonal three-phase checkerboard

Yu. V. Obnosov [1]

Abstract

A two-dimensional doubly-periodic, three-phase hexagonal structure is considered. The flow in the structure is generated by three sets of vortexes/sinks/sources, which are the same in each phase and are located in the centers of the hexagons. Complex analysis methods are utilized to reduce the doubly periodic R-linear conjugation problem to the simpler one, Riemann-Hilbert (RH) problem, on a three-sheeted Riemann surface. In turn, the latter problem is reduced to a RH problem involving three joined sectors on the plane, which was previously investigated in [3]. The limiting cases with one non-conducting phase and two phases of the same conductivities are investigated.

All solutions derived are verified both numerically and analytically. Examples of relevant flow networks, streamlines and equipotentials, are plotted in the whole structure and separately in each phase.

Key words:Composite materials, doubly periodic structure, complex analysis, piece-wise meromorphic solution, conformal mapping

1 Introduction

In this paper we study a planar two-dimensional doubly-periodic three-phase heterogeneous structure. Multi-phase composites, as vital in modern engineering and physics, are the subject of many studies both theoretical and numerical. The main efforts of scientists studying the subject are aimed at determining so-called effective parameters of composites. We are not going to review the area, just mention one of the first work [20], the comprehensive book [10], and later works [5, 6, 13, 11].

More difficult and much more rare are works in which explicit solutions for the field variables are found. This problem was solved for a field generated by a dipole at infinity for two-, three- and four-phase rectangular checkerboards ([7, 1, 14, 2]), as well as for two-phase circular, triangular and three-phase rhomboidal doubly-periodic structures ([12, 15, 3]).

The papers [16, 17, 18, 19, 4, 8] deal with the fields that are generated by arbitrary vorteces/sinks/sourses in some simple model composites.

The ideas of the last two groups of works are combined in the present paper. Namely, we consider hexagonal three–phase tessellation with three sets of vorteces/sinks/sourses, the same in each phase, which generate a field in the structure. Mathematically, this problem relies upon the Markushevich problem (the problem of $\mathbb{R}$-linear conjugation or the generalized Riemann problem), which ultimately can be reduced to the RH problem for three joined sectors. Exactly the same RH problem was considered in [3] for a non-trivial geometry (see Figure 1) constructed from diamonds.

Figure 1: The 3-phased regular diamond structure.

[1]Professor, Institute of Mathematics and Mechanics, Kazan Federal University, Kremlevskaja Str., 35, 420008, Kazan, Russia (yobnosov@kpfu.ru).

The paper is organized as follows: We formulate the problem, and set forth our notation in section 2(2.1). Then the tessellated structure is reduced to a much simpler, three joined sectors, problem using conformal mappings (subsection 2.2). It turned out that the last problem exactly coincided with the earlier studied in [3]. This made it possible to immediately write down the general solution of the set boundary value problem (subsection 2.3). The solvability conditions and the unique solution satisfying some additional requirements are found in subsection 2.4. Some examples of relevant flow networks, streamlines and equipotentials, are given in subsection 2.5. The limiting case of a two phase structure is studied in section 3. Some concluding remarks are summarized together in section 4.

2 The three-phased double-periodic structure

We consider three-phase, piecewise continuous, doubly-periodic, linear media (see Fig. 2) whose stationary physical fields can be represented in terms of a vector field that is both solenoidal and irrotational; this encompasses several physical scenarios in hydrology, electro- or magneto-statics, heat flow, and elasticity. The language of hydrology is used in later

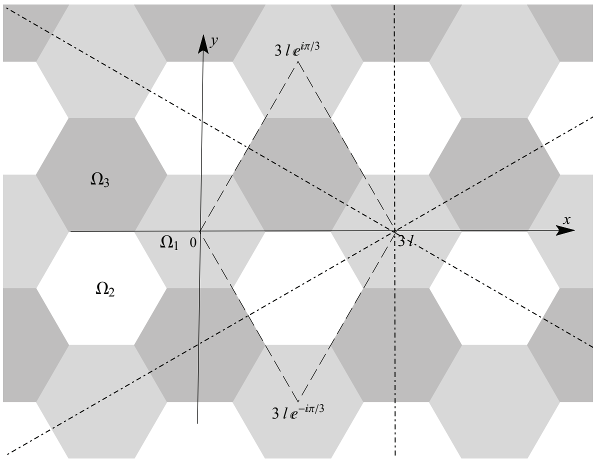

Figure 2: The 3-phased regular hexagonal structure.

sections. In each phase, distinguished by the subscript j where $j = 1, 2, 3$, we define a vector field $\mathbf{v}_j = (v_{jx}, v_{jy})$ of the horizontal and vertical components v_x, v_y such that both

$$\nabla \cdot \mathbf{v}_k = 0, \qquad \nabla \times \mathbf{v}_k = 0.$$

We will utilize complex variables, that is, $z = x + \mathrm{i}\,y$. In each phase, Ω_j, piecewise meromorphic functions $v_j(z) = v_{jx} - \mathrm{i}\,v_{jy}$ are defined ($j = 1, 2, 3$). The continuity boundary conditions between each phase are that the normal components of $\mathbf{v}_j$ are continuous across each boundary, and that the tangential components of $\rho_j \mathbf{v}_j$ are similarly continuous; the constant parameters ρ_j correspond to a phase property of each medium. In the terminology of hydrology we have the Darcian velocity vector $\mathbf{v} = v_x + \mathrm{i} v_y = -k\nabla h$ with $h(x, y)$ as the hydraulic head and k is the hydraulic conductivity. The phase property ρ is the resistivity, and it is $1/k$.

The flow is generated by three sets of vortexes/sources/sinks, which are identical in each phase and located at the hexagons centers.

2.1 Formulation

Each of the three phases Ω_j of the composite structure we are studying consists of an infinite number of hexagons, each with sides length l and vertex angles $2\pi/3$. Through the center of each hexagon go three symmetry axes of the whole structure. These axes form three sets of parallel straight lines, one is perpendicular to the real axes, and the others cross it subtending angles $-\pi/6$ and $\pi/6$ with the real axis (see dot-dashed lines in Fig. 2). Let $\mathcal{L}$ be the set of all intervals forming interface of our structure. $\mathcal{L}$ consists of three subsets $\mathcal{L}_j$, which are the unions of all intervals going under the angle $(j-1)\pi/3$ to the real axis for $j = 1, 2, 3$ respectively. In its turn, $\mathcal{L}_j = \mathcal{L}_{j1} \cup \mathcal{L}_{j2} \cup \mathcal{L}_{j3}$ and $\mathcal{L}_{jk}$ is the set of corresponding intervals along which are conjugated phases Ω_k and Ω_{k+1}, $k = 1, 2, 3$ (here and everywhere below subindex 4 has to be identified with subindex 1)

Using the continuity boundary conditions between each phase, we write the boundary value problem as

$$\mathrm{Re}\,[\varepsilon^{j-1}(\rho_k v_k(t) - \rho_{k+1} v_{k+1}(t)] = 0, \ \mathrm{Im}\,[\varepsilon^{j-1}(v_k(t) - v_{k+1}(t)] = 0, \quad t \in \mathcal{L}_{jk}, \tag{1}$$

where $k = 1, 2, 3$, $j = 1, 2, 3$, $\varepsilon = \mathrm{e}^{\mathrm{i}\,\pi/3}$ and remind that $v_4(z) \equiv v_1(z)$.

Last two real conditions are equivalent to the following single complex boundary condition

$$v_k(t) = A_k v_{k+1}(t) - B_k \bar{\varepsilon}^{2(j-1)} \overline{v_{k+1}(t)}, \quad t \in \mathcal{L}_{jk}, \quad k = 1, 2, 3, \ j = 1, 2, 3, \tag{2}$$

where

$$A_k = \frac{\rho_k + \rho_{k+1}}{2\rho_k}, \quad B_k = \frac{\rho_k - \rho_{k+1}}{2\rho_k}, k = 1, 2, 3 \quad (\rho_4 = \rho_1). \tag{3}$$

Our structure is the doubly-periodic one it has two primitive periods $2\omega = 3l\varepsilon$ and $2\omega' = 3l\bar{\varepsilon}$, it's elementary cell is the parallelogram (rhombus) bounded by dashed lines in Fig. 2; we use the same Ω for each portion of a particular phase, i.e. Ω_j are the all hexagons the resistivity of which is ρ_j as well as every one representative of this set ($j = 1, 2, 3$). A piece-wise meromorphic solution of the problem (2) may have integrable singularities at the vertices of hexagons, and there should be simple poles at their centers, such that

$$\mathrm{res}_{O_j} v_j(z) = \frac{Q_j - \mathrm{i}\Gamma_j}{2\pi}, \qquad j = 1, 2, 3, \tag{4}$$

where O_j is the center of Ω_j, Q_j is the sink/source strength, Γ_j is the vortex intensity. Below it will be shown that only two of the three pairs (Q_j, Γ_j) can be fixed in advance.

Thus, it is required to find a piecewise meromorphic doubly periodic, with primitive periods $2\omega = 3l\varepsilon$ and $2\omega' = 3l\bar{\varepsilon}$, solution $v(z) = v_k(z)$, $z \in \Omega_k$ of the boundary-value problem (1) having integrable singularities at corner points of the interface and satisfying the conditions (4).

2.2 Conformal mapping

Below, instead of the elementary cell, we consider the union Ω of three adjacent hexagons Ω_1, Ω_2, Ω_3 (see Fig. 3). The coinciding second subindex in the designation of the vertices A_{kj} means that the corresponding vertices coincide or congruent (differ by a period).

We begin with a conformal mapping of the sector $\{\zeta : 0 < \arg\zeta < \pi/3\}$ onto the triangle with vertices A_{11}, O_1, A_{16}, which are mapped to $(0, 1, \infty)$. The required mapping gives the Schwarz-Christoffel integral

$$z(\zeta) = \frac{l\Gamma(2/3)}{\Gamma(1/3)^2} \int_0^{\zeta^3} \frac{\mathrm{d}t}{t^{2/3}(1-t)^{2/3}} - l. \tag{5}$$

Using the definition of the hypergeometric function, the last integral is identified as

$$z(\zeta) = \frac{3l\Gamma(2/3)\zeta}{\Gamma(1/3)^2} \mathrm{F}(1/3, 2/3; 4/3; \zeta^3) - l.$$

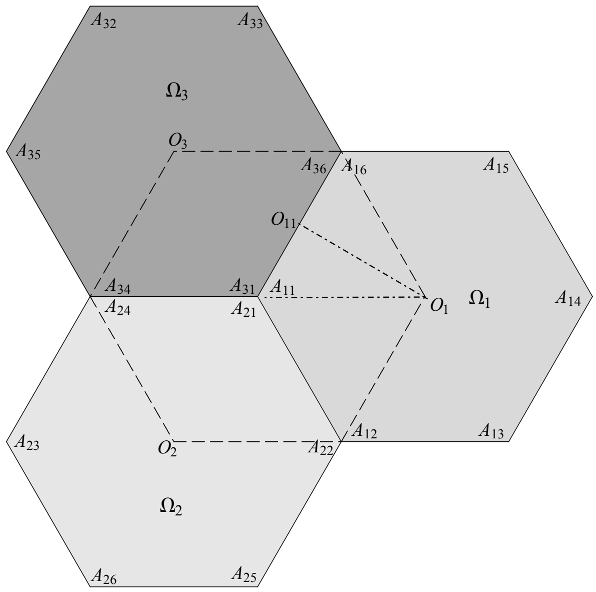

Figure 3: Three adjacent hexagons (an analogue of the elementary cell)

We use successive analytic continuations of the function $z(\zeta)$, via the Riemann-Schwartz symmetry principle, at first across the interval $(0, 1)$ and then across both sides of the cut along the ray $(1, \infty)$. The continued function gives a conformal mapping of the three-sheeted sector, the sheets of which are glued together as shown in Fig. 4, onto the hexagon Ω_1 (here and below, the same notations are used for images and preimages). Further continuation of $z(\zeta)$ through each of the sides (A_{11}, A_{12}) and (A_{11}, A_{16}) is defined on a three-sheeted Riemann surface with cuts along the rays $\{\zeta; \arg\zeta = (2k+1)\pi/3\}$, $k = 0, 1, 2$ on the second and third sheets. This surface is mapped by the function $z(\zeta)$ onto Ω. Note that opposite sides of cuts correspond to congruent sides of Ω. We identify congruent sides of Ω and glue correspondingly sides of cuts. Thus we obtain a closed three-sheeted Riemann surface $\mathfrak{R}_\zeta$.

Consider the inversion $\zeta(z)$ (not to be confused with the Weierstrass ζ-function) of the function obtained by all possible analytic continuations of the function (5). Clearly, that if $\zeta(z)$ is defined in Ω_1 then

$$\zeta(z) = \bar{\varepsilon}^2 \overline{\zeta(\bar{\varepsilon}^2 \overline{(z - O_2)})} \quad \text{and} \quad \zeta(z) = \varepsilon^2 \overline{\zeta(\varepsilon^2 \overline{(z - O_3)})} \tag{6}$$

are its analytic continuations into Ω_2 and Ω_3, respectively. The subsequent doubly-periodic extension from Ω to the whole plane gives the function $\zeta(z)$, which is an elliptic function with primitive periods 2ω, $2\omega'$ and simple zeros and poles at all points congruent with A_{11}, A_{13}, A_{15} and A_{12}, A_{14}, A_{16}, respectively. Hence, under the condition $\zeta(0) = 1$, we obtain ([9], p.227)

$$\zeta(z) = -\frac{\sigma(z+l)\sigma(z-l\varepsilon)\sigma(z-l\bar{\varepsilon})}{\sigma(z-l)\sigma(z+l\varepsilon)\sigma(\zeta+l\bar{\varepsilon})}, \tag{7}$$

where $\sigma(z) = \sigma(z; \omega, \omega')$ is the Weierstrass σ-function with primitive periods 2ω, $2\omega'$. Note that the sum of zeros of $\zeta(z)$ within the parallelogram of periods equals the sum of its poles. The function (7) maps conformally the domain Ω onto the Riemann surface $\mathfrak{R}_\zeta$ (see Fig. 4).

The mapping function (7) saves angles at all vertices A_{kj} and satisfies the conditions:

$$\begin{aligned} &\varepsilon^{2(k-1)}\overline{\zeta(\varepsilon^{2(j-1)}\overline{(z-O_k)} + O_k)} \equiv \zeta(z),\ \overline{\zeta(\varepsilon^{2j-1}\overline{(z-O_k)} + O_k)} \equiv 1/\zeta(z), \\ &\zeta(2O_k - z) \equiv \varepsilon^{2(k-1)}/\zeta(z),\ \zeta(\varepsilon^{\pm 2}(z-O_k) + O_k) \equiv \zeta(z),\ j,k = 1,2,3. \end{aligned} \tag{8}$$

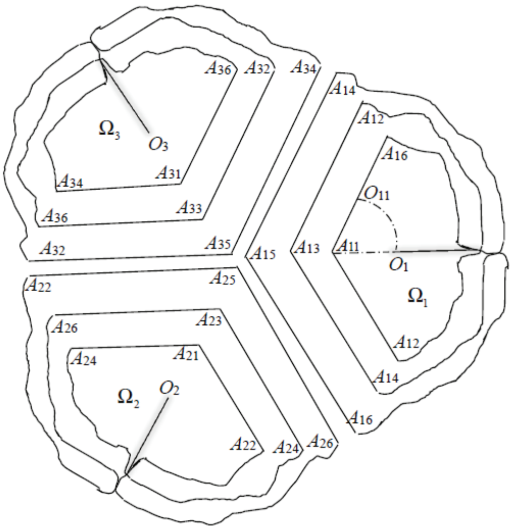

Figure 4: The image of the domain Ω under the mapping by function (7)

The first identity (8) means that the values of the function (7) at points symmetric about diagonals of the hexagon Ω_k are symmetric with respect to bisectrix of the three–sheeted sector Ω_k in the ζ-plane. Its validity is a direct consequence of the method of the analytic continuation through which the mapping function (7) was obtained.

The second identity (8) connects the values of the function (7) at two points symmetric about the perpendiculars from the center O_k to the sides of the hexagon Ω_k. To prove this identity, it is sufficient to take into account that the same function (7) can be obtained if we start from the triangle $A_{11}O_{11}O_1$ (see Fig. 3). We map this triangle on the curvilinear triangle $A_{11}O_{11}O_1$ with (O_{11}, O_1) being the arc of the unit circle (see Fig. 4). Then the Riemann-Schwarz symmetry principle gives such an analytic continuation through the side (O_{11}, O_1) of the mapping function, which satisfies the second identity (8).

The third identity (8) connects the values of the function (7) at two points that are symmetric about the center O_k of the hexagon Ω_k. This identity follows from the first two identities (8), since $2O_k - z = \varepsilon^{2(k-1)}(\overline{((\varepsilon^{2l-1}\overline{(z-O_k)}+O_k)-O_k)}+O_k)$ if $k-l=2$.

The last identity (8) means that the function (7) takes the equal values at three points, which are obtained from each other by rotating through an angle $2\pi/3$ relative to the center O_k. The required identity is the result of the dual application of the first identity (8) using the representation $\varepsilon^{\pm2}(z-O_k)+O_k = \varepsilon^{2(m-1)}(\overline{((\varepsilon^{2(l-1)}\overline{(z-O_k)}+O_k)-O_k)}+O_k)$ if $m-l=\pm2$.

The Taylor series expansion of the function (7) in a neighborhood of the center O_k, by virtue of the first identity (8) and (6), has the form

$$\zeta(z) = \overline{\varepsilon}^{2(k-1)}\left(1+\sum_{k=1}^{\infty}\zeta_k(z-O_k)^{3k}\right), \quad z\in\Omega_k, \quad k=1,2,3, \tag{9}$$

where all ζ_k are real.

Below, along with (7), the following function will be used:

$$\mu(z) = \sqrt[3]{1-\zeta(z)^3}. \tag{10}$$

Function (10) maps the domain Ω onto the three-sheeted Riemann surface $\mathfrak{R}_\mu$. Each hexagon Ω_k is mapped by this function onto the whole plane with three cuts along the rays $\{z : |z| > 1, \arg z = 2\pi j/3\}$, $j = 0, 1, 2$ (see Fig. 5). The surface $\mathfrak{R}_\mu$ consists of these three sheets with

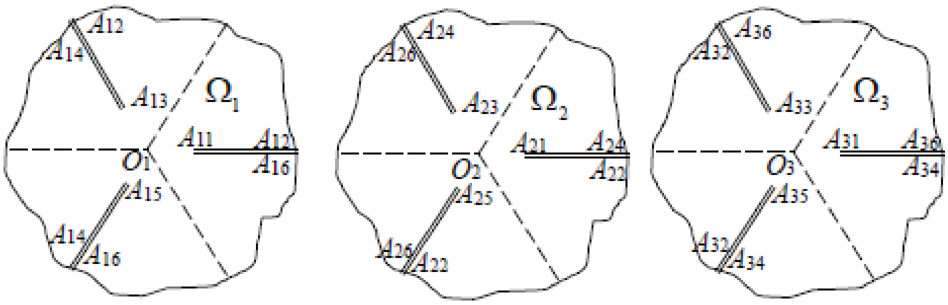

Figure 5: The image of the domain Ω under the mapping by function (10)

crosswise glued sides of the cuts in accordance with the double periodicity of the functions (7), (10).

Let us consider more thoroughly the properties of the function (10). In view of the nature of the conformal mapping realized by the function (10), it follows that

$$\mu(z) \equiv \varepsilon^2 \overline{\mu(\varepsilon^2 \overline{z})} \equiv \overline{\varepsilon}^2 \overline{\mu(\overline{\varepsilon}^2 \overline{z})} \equiv \varepsilon^{\mp 2} \mu(\varepsilon^{\pm 2} z). \tag{11}$$

The Taylor series expansion of the function (10) in a neighborhood of the origin, by virtue of the identities (11), has the form

$$\mu(z) = z \sum_{k=0}^{\infty} \mu_k z^{3k}, \tag{12}$$

where all μ_k are real and, in particular,

$$\mu_0 = \sqrt[3]{-\zeta'''(0)/2} = -1.7666387502854504`. \tag{13}$$

Analytic continuation of the function $\mu(z)$ from Ω_1 to Ω_k ($k = 2, 3$) obtained by the Riemann-Schwarz symmetry principle are

$$\mu(z) = \overline{\mu(\overline{\varepsilon}^{2(k-1)}(\overline{z} + l) - l)} = \overline{\mu(\overline{\varepsilon}^{2(k-1)}(\overline{z} - \overline{O}_k)}, \quad z \in \Omega_k. \tag{14}$$

Due to (12), (14) we get

$$\mu(z) = \varepsilon^{2(k-1)}(z - O_k) \sum_{k=0}^{\infty} \mu_k (z - O_k)^{3k}, \quad z \in \Omega_k, \quad k = 1, 2, 3. \tag{15}$$

At last, the function (10) maps conformally $\mathfrak{R}_\zeta$ onto $\mathfrak{R}_\mu$ and

$$\mu((\zeta, 2)) = \varepsilon^2 \overline{\mu((\overline{\zeta}, 1))}, \quad \mu((\zeta, 3)) = \overline{\varepsilon}^2 \overline{\mu((\overline{\zeta}, 1))}, \tag{16}$$

where (ζ, k) is the point ζ at the k-th sheet of $\mathfrak{R}_\zeta$.

Summarising, the function $\mu(\zeta)$ has the following properties:
1. $\mu(\zeta)$ has simple pole at infinity;
2. $\mu(\zeta(z))$ has simple zeros at all centers $O_{1,2,3}$;
3. $\Im \mu((\overline{\varepsilon}^{2k-1}\xi, 1)) = 0$ for $\xi > 0$, $k = 1, 2, 3$ and, hence, $\Im\big(\overline{\varepsilon}^2 \mu((\overline{\varepsilon}^{2k-1}\xi, 2))\big) = 0$, $\Im\big(\varepsilon^2 \mu((\overline{\varepsilon}^{2k-1}\xi, 3))\big) = 0$ due to (16).

2.3 Solution of the problem (1)

Due to the double periodicity of the required function $v(z)$ boundary conditions (2) are that

$$\begin{array}{ll}
v_1(t) = A_1 v_2(t) - B_1\varepsilon^2\overline{v_2(t)}, & t\in(A_{11},A_{12}),\\
v_2(t) = A_2 v_3(t) - B_2\overline{v_3(t)}, & t\in(A_{21},A_{24}),\\
v_3(t) = A_3 v_1(t) - B_3\overline{\varepsilon}^2\overline{v_1(t)}, & t\in(A_{11},A_{16}),\\
v_1(t) = A_1 v_2(t-3l) - B_1\overline{\varepsilon}^2\overline{v_2(t-3l)}, & t\in(A_{13},A_{14}),\\
v_2(t) = A_2 v_3(t+3l\varepsilon) - B_2\varepsilon^2\overline{v_3(t+3l\varepsilon)}, & t\in(A_{23},A_{26}),\\
v_3(t-3l\overline{\varepsilon}) = A_3 v_1(t) - B_3\overline{v_1(t)}, & t\in(A_{12},A_{13}),\\
v_1(t) = A_1 v_2(t-3l\varepsilon) - B_1\overline{v_2(t-3l\varepsilon)}, & t\in(A_{15},A_{16}),\\
v_2(t) = A_2 v_3(t-3l\overline{\varepsilon}) - B_2\overline{\varepsilon}^2\overline{v_3(t-3l\overline{\varepsilon})}, & t\in(A_{22},A_{25}),\\
v_3(t-3l) = A_3 v_1(t) - B_3\varepsilon^2\overline{v_1(t)}, & t\in(A_{14},A_{15}).
\end{array} \tag{17}$$

Now we introduce the following function

$$w(\zeta) = \zeta\mu(\zeta)v[z(\zeta)] = w_k(\zeta), \quad \zeta\in\Omega_k, \quad k=1,2,3. \tag{18}$$

This function is a piece-wise holomorphic function defined on the Riemann surface $\mathfrak{R}_\zeta$. According to (17) and the properties of the function $\mu(\zeta)$ listed above, $w(\zeta)$ satisfies the identical boundary conditions on all three sheets of the Riemann surface $\mathfrak{R}_\zeta$. Namely,

$$w_k(\overline{\varepsilon}^{2k-1}\xi) = A_k w_{k+1}(\overline{\varepsilon}^{2k-1}\xi) - B_k\overline{w_{k+1}(\overline{\varepsilon}^{2k-1}\xi)}, \quad \xi>0, \quad k=1,2,3, \tag{19}$$

where $w_4(\zeta)\equiv w_1(\zeta)$. The remarkable fact is that the boundary conditions (19) exactly coincide with conditions (A1) in [3], if the latter are rewritten in a complex form.

We require a piece-wise holomorphic solution of the problem (19) that vanishes at $\zeta=0$, and all functions $w_j(\zeta)$ should have at $\zeta=\infty$ a singularity less than 3. The solution of problem (19) was obtained in [3] in the same class of functions with a single difference only in the condition at infinity, where $w_j(\zeta)$ should have a singularity less than 3/2.

Just repeating all steps in finding a solution of problem (A1) in [3] we will obtain a general solution of problem (19) as a linear combination of four linear independent particular solutions, namely

$$\begin{aligned}
v_1(z) &= \Big(c_1A_1^+\zeta^{3\alpha^+-1} + c_2\overline{A_1^+}\zeta^{2-3\alpha^+} + \\
&\qquad +\mathrm{i}\,(c_3A_1^-\zeta^{3\alpha^--1} + c_4\overline{A_1^-}\zeta^{2-3\alpha^-})\Big)/\mu(\zeta), \quad z\in\Omega_1,\\
v_2(z) &= \Big(c_1A_2^+\lambda_+^2\zeta^{3\alpha^+-1} + c_2\overline{A_2^+}\overline{\lambda}_+^2\zeta^{2-3\alpha^+} + \\
&\qquad +\mathrm{i}\,(c_3A_2^-\lambda_-^2\zeta^{3\alpha^--1} + c_4\overline{A_2^-}\overline{\lambda}_-^2\zeta^{2-3\alpha^-})\Big)/\mu(\zeta), \quad z\in\Omega_2,\\
v_3(z) &= \Big(c_1A_3^+\overline{\lambda}_+^2\zeta^{3\alpha^+-1} + c_2\overline{A_3^+}\lambda_+^2\zeta^{2-3\alpha^+} + \\
&\qquad +\mathrm{i}\,(c_3A_3^-\overline{\lambda}_-^2\zeta^{3\alpha^--1} + c_4\overline{A_3^-}\lambda_-^2\zeta^{2-3\alpha^-})\Big)/\mu(\zeta), \quad z\in\Omega_3,
\end{aligned} \tag{20}$$

where c_j are, at this stage, arbitrary real parameters; $\zeta=\zeta(z)$ and $\mu(\zeta)$ are determined by the equations (7) and (10), respectively; the branch of the analytic function ζ^γ is fixed onto each sheet of $\mathfrak{R}_\zeta$ with a cut along the negative part of the real axis by the condition $|\arg\zeta|<\pi$; the terms A_j^+, A_j^-, $j=1,2,3$ are given by the equations

$$\begin{aligned}
A_1^+ &= -(1-c)(\Delta+a)\lambda_+ - (1+a)(\Delta-c)\overline{\lambda}_+,\\
A_2^+ &= (1+a)[(\Delta-c)\lambda_+ + b(1-c)\overline{\lambda}_+],\\
A_3^+ &= (1-c)[(\Delta+a)\overline{\lambda}_+ - b(1+a)\lambda_+];
\end{aligned} \tag{21}$$

$$\begin{aligned}
A_1^- &= (1+c)(\Delta+a)\lambda_- + (1-a)(\Delta-c)\overline{\lambda}_-,\\
A_2^- &= -(1+a)[(\Delta-c)\lambda_- + b(1+c)\overline{\lambda}_-],\\
A_3^- &= -(1-c)[(\Delta+a)\overline{\lambda}_- - b(1-a)\lambda_-];
\end{aligned} \tag{22}$$

in its turn

$$a = \Delta_{12}, \quad b = \Delta_{23}, \quad c = \Delta_{31}, \qquad \Delta_{pq} = \frac{\rho_p - \rho_q}{\rho_p + \rho_q}; \tag{23}$$

and

$$\Delta = \sqrt{-ab - bc - ac}; \tag{24}$$

$$\lambda_\pm = \mathrm{e}^{\mathrm{i}\,\pi\alpha^\pm} = \frac{\sqrt{1 \mp \Delta}}{2} + \frac{\mathrm{i}}{2}\sqrt{3 \pm \Delta}, \quad \alpha^\pm = \frac{1}{\pi} \arccos \frac{\sqrt{1 \mp \Delta}}{2}. \tag{25}$$

According (23), (24)

$$\Delta^2 = -(ab + bc + ca) = \frac{\rho_1(\rho_2 - \rho_3)^2 + \rho_2(\rho_3 - \rho_1)^2 + \rho_3(\rho_1 - \rho_2)^2}{(\rho_1 + \rho_2)(\rho_2 + \rho_3)(\rho_3 + \rho_1)} \geq 0,$$

$$1 - \Delta^2 = \frac{(1 - a^2)(1 - c^2)}{1 + ac} \geq 0,$$

and we take $0 \leq \Delta \leq 1$. This constrains us to have $0 \leq 3\alpha^+ - 1 \leq 1/2$, $1/2 \leq 2 - 3\alpha^+ \leq 1$ and $-1/4 \leq 3\alpha^- - 1 \leq 0$, $1 \leq 2 - 3\alpha^- \leq 5/4$.

2.4 Solution of the problem (1), (4)

The real parameters c_j, $j = 1, 2, 3, 4$ in the general solution (22) should be defined using the conditions (4).

In accordance with the above fixed branch of the function ζ^γ, we must take

$$\zeta(O_1) = 1, \quad \zeta(O_2) = \bar{\varepsilon}^2 = \exp(-2\pi\mathrm{i}/3), \quad \zeta(O_3) = \varepsilon^2 = \exp(2\pi\mathrm{i}/3).$$

Then from (9), (12), (13), (15), (20) through (25) follows

$$\mathrm{res}_{O_k} v_k(z) = \left(d_1 \Re A_k^+ - d_4 \Im A_k^- + \mathrm{i}(d_2 \Im A_k^+ + d_3 \Re A_k^-)\right)/\mu_0, \quad k = 1, 2, 3,$$

here $d_1 = c_1 + c_2$, $d_2 = c_1 - c_2$, $d_3 = c_3 + c_4$, $d_4 = c_3 - c_4$. Using the conditions (4) we obtain

$$\begin{aligned} d_1 \Re A_k^+ - d_4 \Im A_k^- &= Q_k \mu_0/(2\pi), \quad k = 1, 2, 3, \\ d_2 \Im A_k^+ + d_3 \Re A_k^- &= -\Gamma_k \mu_0/(2\pi), \quad k = 1, 2, 3. \end{aligned} \tag{26}$$

An important consequence of the equalities (26) is the following statement.

Theorem 1. *The strengths, Q_j, and the intensities, Γ_j, of vortexes–sinks/sources satisfy the relations*

$$Q_1 + Q_2 + Q_3 = 0, \qquad \rho_1\Gamma_1 + \rho_2\Gamma_2 + \rho_3\Gamma_3 = 0. \tag{27}$$

Proof. The first of these relations, evident from physical point of view, serves as an indirect confirmation of the correctness of the solution (20). To prove both relations (27) it is sufficient to show that

$$\sum_{k=1}^{3} \Re A_k^+ = 0, \qquad \sum_{k=1}^{3} \Im A_k^- = 0,$$

$$\sum_{k=1}^{3} \rho_k \Im A_k^+ = 0, \qquad \sum_{k=1}^{3} \rho_k \Re A_k^- = 0,$$

where A_k^+, A_k^- are defined in (21), (22). To prove the last four equalities, one can use symbolic munipulations in the Mathematica package [21].

We obtain the assertion of our theorem for Q_j by summing the first three equations (26). Multiplying the corresponding second equation (26) by ρ_k and summing up the results, we obtain the second relation of the theorem.

Remark 1. The conditions (27) are necessary and, as will be shown below, are sufficient for the unique solvability of the problem (2), (4).

Remark 2. It is quite natural to assume that the first equality (27) will be valid for an arbitrary location of vortex–sinks/sourcies in the hexagons Ω_j. On physics ground, this equality, or rather its generalization, holds for any double-periodic n-phase heterogeneous structure. As for the second equality (27), we can assume that it also does not depend on the vortex–sinks/sourcies location and geometry of the regular structure, but it requires strict physical or mathematical proof.

The equations (26) with $k = 1, 2$ give two systems of linear equations with respect to parameters d_1, d_4 and d_2, d_3. Both these systems are uniquely solvable as their determinants

$$D_1 = \Re A_2^+ \Im A_1^- - \Re A_1^+ \Im A_2^-, \quad D_2 = \Im A_1^+ \Re A_2^- - \Im A_2^+ \Re A_1^-$$

differ from zero if $\rho_2 \neq \rho_3$. To prove this, one has to use (21) through (25) and present $D_{1,2}$ as second-order polynomials with respect to Δ (up to non-vanishing positive factors). Discriminants of the last polynomials are

$$-4\rho_1\rho_2\rho_3(\rho_2 - \rho_3)^2(\rho_1 + \rho_2 + \rho_3), \quad -4\rho_1^2(\rho_2 - \rho_3)^2(\rho_1\rho_2 + \rho_1\rho_3 + \rho_2\rho_3),$$

respectively (we omit the tedious algebraic transformations that were carried out using symbolic manipulations in the Mathematica package with further simplifications). Thus, both discriminants are negative, this proves our assertion. The case $\rho_2 = \rho_3$ will be considered later.

The parameters d_j are

$$\begin{aligned} d_1 &= \frac{\mu_0}{2\pi D_1}\left(Q_2 \Im A_1^- - Q_1 \Im A_2^-\right), \quad d_4 = \frac{\mu_0}{2\pi D_1}\left(Q_2 \Re A_1^+ - Q_1 \Re A_2^+\right), \\ d_2 &= \frac{\mu_0}{2\pi D_2}\left(\Gamma_2 \Re A_1^- - \Gamma_1 \Re A_2^-\right), \quad d_3 = \frac{\mu_0}{2\pi D_2}\left(\Gamma_1 \Im A_2^+ - \Gamma_2 \Im A_1^+\right). \end{aligned} \tag{28}$$

Then the required parameters c_j are

$$c_1 = \frac{d_1 + d_2}{2}, \quad c_2 = \frac{d_1 - d_2}{2}, \quad c_3 = \frac{d_3 + d_4}{2}, \quad c_4 = \frac{d_3 - d_4}{2}. \tag{29}$$

This completes the solution of the problem posed.

The following statement is proved.

Theorem 2. *If the solvability conditions* (27) *are met and* $\rho_2 \neq \rho_3$ *then the problem* (2), (4) *has the unique solution* (20), *where parameters* c_j *are defined in* (28), (29).

Concluding this section, we consider the limit case $\rho_1 = \infty$, that is, the first phase Ω_1 is non-conducting and, naturally, $Q_1 = \Gamma_1 = 0$. Passing to the limit $\rho_1 \to \infty$ in the relations (20) through (25) we obtain $a = -c = \Delta = 1$ and

$$\begin{aligned} &v_1(z) \equiv 0, \quad z \in \Omega_1, \\ &v_2(z) = \mathrm{i}\left(c_1(1-b)\zeta^{1/2} + c_2 \mathrm{e}^{-\mathrm{i}\pi/4}\zeta^{-1/4} + c_3 \mathrm{e}^{\mathrm{i}\pi/4}\zeta^{5/4}\right)/\mu(\zeta), \quad z \in \Omega_2, \\ &v_3(z) = \mathrm{i}\left(-c_1(1+b)\zeta^{1/2} + c_2 \mathrm{e}^{\mathrm{i}\pi/4}\zeta^{-1/4} + c_3 \mathrm{e}^{-\mathrm{i}\pi/4}\zeta^{5/4}\right)/\mu(\zeta), \; z \in \Omega_3, \end{aligned} \tag{30}$$

where real parameters c_j must be defined from the conditions (4) for $j = 2, 3$. That results in the following system of linear equations:

$$\operatorname{res}_{O_2} v_2(z) = -\left(\mathrm{i}\left[(1-b)c_1 + \frac{\sqrt{2}}{2}(c_2 + c_3)\right] + \frac{\sqrt{2}}{2}(c_2 - c_3)\right)/\mu_0 = \frac{Q_2 - \mathrm{i}\Gamma_2}{2\pi},$$

$$\operatorname{res}_{O_3} v_3(z) = \left(\mathrm{i}\left[(1+b)c_1 - \frac{\sqrt{2}}{2}(c_2 + c_3)\right] + \frac{\sqrt{2}}{2}(c_2 - c_3)\right)/\mu_0 = \frac{Q_3 - \mathrm{i}\Gamma_3}{2\pi}.$$

A comparison of the real parts in the last two equations gives the necessary solvability condition: $Q_2 = -Q_3$, as of course it should on physical grounds. If $Q_2 = -Q_3$ then the last system has the unique solution

$$c_1 = \frac{\mu_0(\Gamma_2 - \Gamma_3)}{4\pi}, \quad c_{2,3} = \frac{\mu_0((1+b)\Gamma_2 + (1-b)\Gamma_3 \pm 2Q_2)}{4\sqrt{2}\pi}. \tag{31}$$

Thus, the following theorem holds.

Theorem 3. *If $\rho_1 = \infty$ and $Q_2 = -Q_3$ then the problem* (2), (4) *has the unique solution* (30), *where parameters c_j are defined in* (31).

2.5 Examples

This section provides examples of flow nets. First, streamlines (solid lines with arrows) and equipotential lines (dashed lines) are represented in the entire structure. Below are given the zoomed pictures of streamlines in phases 1,2,3, respectively.

Fig. 6 illustrates the case of no sinks/sources, but with two given vortices at the centers O_1, O_2 and the corresponding generated vortex in O_3.

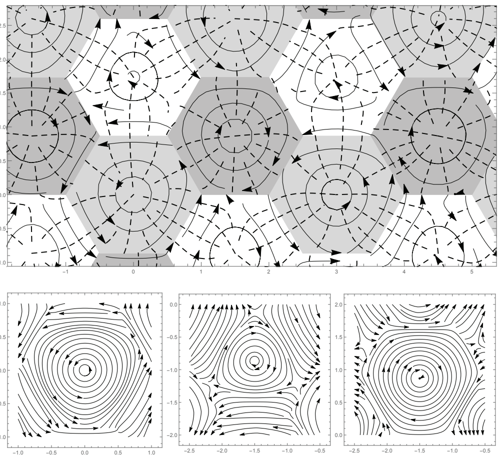

Figure 6: $\rho_1 = 1$, $\rho_2 = 5$, $\rho_3 = 0.2$, $Q_1 = 0$, $Q_2 = 0$, $\Gamma_1 = 3$, $\Gamma_2 = -3$

The case of a sink in O_1 and a source in O_2 of equal strengths is presented in the Fig. 7. Center O_3 is the stagnation point on this occasion.

Fig. 8 shows the case of vortex–sinks/sources in O_1, O_2 such that $Q_1 = 5$, $Q_2 = -3$, $\Gamma_1 = -3$, $\Gamma_2 = 5$. Here, in accordance with (27), we have a vortex–sink in the center of the hexagon Ω_3 with a strength $Q_3 = -2$ and a very high intensity $\Gamma_3 = -470$, which generates three stagnation points in Ω_1.

Two cases of a non conducting first phase are presented in Fig. 9.

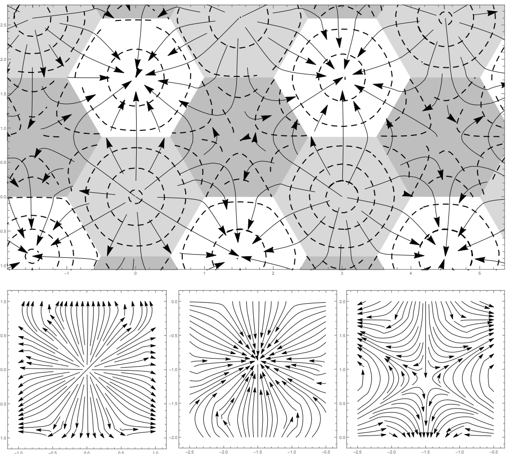

Figure 7: $\rho_1 = 1$, $\rho_2 = 10$, $\rho_3 = 0.1$, $Q_1 = 1$, $Q_2 = -1$, $\Gamma_1 = 0$, $\Gamma_2 = 0$

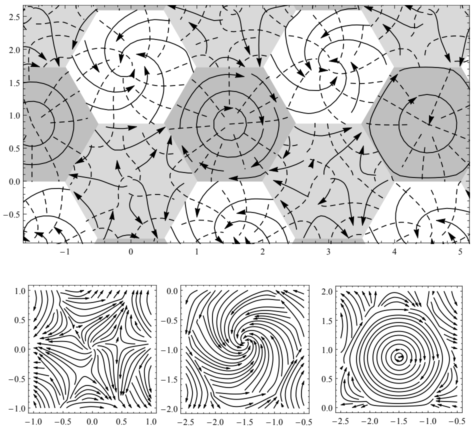

Figure 8: $\rho_1 = 1$, $\rho_2 = 10$, $\rho_3 = 0.1$, $Q_1 = 5$, $Q_2 = -3$, $\Gamma_1 = -3$, $\Gamma_2 = 5$

3 Two equal neighboring phases: $\rho_2 = \rho_3$

The limiting case $\rho_2 = \rho_3$ for the problem (19) was considered in [3], by which we now get a general solution of the form

$$\begin{aligned} v_1(z) &= \Big(-\sqrt{1-a}(c_1\zeta^{3\alpha^+-1} + c_2\zeta^{2-3\alpha^+}) + \\ &\qquad + \mathrm{i}\,\tfrac{\rho_2}{\rho_1}\sqrt{1+a}(c_3\zeta^{3\alpha^--1} + c_4\zeta^{2-3\alpha^-})\Big)/\mu(\zeta), \quad z \in \Omega_1, \\ v_2(z) &= \Big(c_1\lambda_+^3\zeta^{3\alpha^+-1} + c_2\overline{\lambda}_+^3\zeta^{2-3\alpha^+} - \\ &\qquad -\mathrm{i}\,(c_3\lambda_-^3\zeta^{3\alpha^--1} + c_4\overline{\lambda}_-^3\zeta^{2-3\alpha^-})\Big)/\mu(\zeta), \quad z \in \Omega_2, \\ v_3(z) &= \Big(c_1\overline{\lambda}_+^3\zeta^{3\alpha^+-1} + c_2\lambda_+^3\zeta^{2-3\alpha^+} - \\ &\qquad -\mathrm{i}\,(c_3\overline{\lambda}_-^3\zeta^{3\alpha^--1} + c_4\lambda_-^3\zeta^{2-3\alpha^-})\Big)/\mu(\zeta), \quad z \in \Omega_3, \end{aligned} \tag{32}$$

where $\zeta(z)$ are $\mu(\zeta)$ determined in (7) and (10), respectively;

$$\lambda_\pm = \mathrm{e}^{\mathrm{i}\,\pi\alpha^\pm} = \frac{\sqrt{1\mp a}}{2} + \frac{\mathrm{i}}{2}\sqrt{3\pm a}, \quad \alpha^\pm = \frac{1}{\pi}\arccos\frac{\sqrt{1\mp a}}{2}.$$

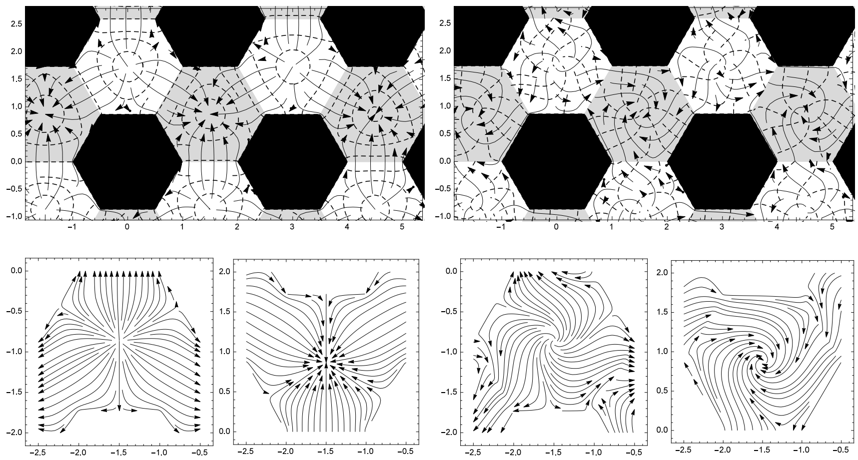

Figure 9: $\rho_1 = \infty$, $\rho_2 = 0.2$, $\rho_3 = 5$, $Q_2 = 2$, $Q_3 = -2$, and $\Gamma_2 = 0$, $\Gamma_3 = 0$ (left panel), $\Gamma_2 = 2$, $\Gamma_3 = -3$ (right panel)

It might appear that there is a contradiction in formulae (32) with, apparently, $v_2(\zeta) \neq v_3(\zeta)$, although physically $v_2(\zeta) \equiv v_3(\zeta)$. But we have to recall that the branches of $\zeta^{3\alpha^\pm-1}$ and $\zeta^{2-3\alpha^\pm}$ are fixed in the ζ–plane with the cut along the negative part of the real axis, i.e. by the condition $-\pi < \arg\zeta < \pi$. With this condition in mind, it is not difficult to see that limit values $v_2(\xi)$ and $v_3(\xi)$ coincide for all $\xi < 0$; thus $v_2(\zeta)$ and $v_3(\zeta)$ in (32) are analytical continuations of each other through $\mathbb{R}^-$.

We assume that the necessary conditions (27) are fulfilled, and we fix the strengths of vortexes–sources/sinks in the phases Ω_2, Ω_3. Due to (9), (15) the residues of the functions (32) at O_2, O_3 are

$$\begin{aligned} 2\mu_0 \mathrm{res}_{O_2} v_2(z) &= d_2\sqrt{1-a} + d_3\sqrt{3-a} + \mathrm{i}(d_1\sqrt{3+a} - d_4\sqrt{1+a}), \\ 2\mu_0 \mathrm{res}_{O_3} v_3(z) &= d_2\sqrt{1-a} - d_3\sqrt{3-a} - \mathrm{i}(d_1\sqrt{3+a} + d_4\sqrt{1+a}), \end{aligned}$$

where $d_1 = c_1 + c_2$, $d_2 = c_1 - c_2$, $d_3 = c_3 + c_4$, $d_4 = c_3 - c_4$. Using (4), we obtain two systems of linear equations with respect to parameters d_2, d_3 and d_1, d_4

$$d_2\sqrt{1-a} + d_3\sqrt{3-a} = Q_2\mu_0/\pi, \quad d_2\sqrt{1-a} - d_3\sqrt{3-a} = Q_3\mu_0/\pi;$$

$$d_1\sqrt{3+a} - d_4\sqrt{1+a} = -\Gamma_2\mu_0/\pi, \quad d_1\sqrt{3+a} + d_4\sqrt{1+a} = \Gamma_3\mu_0/\pi.$$

Both last systems are uniquely solvable. We find their solutions, and then, using (29), we get the parameters c_j

$$\begin{aligned} c_1 &= \frac{\mu_0}{4\pi}\left(\frac{\Gamma_3 - \Gamma_2}{\sqrt{3+a}} + \frac{Q_2 + Q_3}{\sqrt{1-a}}\right), \quad c_2 = \frac{\mu_0}{4\pi}\left(\frac{\Gamma_3 - \Gamma_2}{\sqrt{3+a}} - \frac{Q_2 + Q_3}{\sqrt{1-a}}\right), \\ c_3 &= \frac{\mu_0}{4\pi}\left(\frac{\Gamma_2 + \Gamma_3}{\sqrt{1+a}} + \frac{Q_2 - Q_3}{\sqrt{3-a}}\right), \quad c_4 = \frac{\mu_0}{4\pi}\left(\frac{\Gamma_2 + \Gamma_3}{\sqrt{1+a}} - \frac{Q_2 - Q_3}{\sqrt{3-a}}\right). \end{aligned} \tag{33}$$

Two examples of flow nets, presented in Fig. 10, are obtained by the help of formulae (32), (33).

Concluding this section, we first consider the limit case $\rho_2 = \rho_3$ and $\rho_1 = \infty$. If $\rho_1 = \infty$ then $a = 1$ and from (32) follows $v_1(z) \equiv 0$ and

$$\begin{aligned} v_2(z) &= \mathrm{i}\left(c_1\zeta^{1/2} + c_2 e^{-\mathrm{i}\pi/4}\zeta^{-1/4} + c_3 e^{\mathrm{i}\pi/4}\zeta^{5/4})\right)/\mu(\zeta), \quad z \in \Omega_2, \\ v_3(z) &= \mathrm{i}\left(-c_1\zeta^{1/2} + c_2 e^{\mathrm{i}\pi/4}\zeta^{-1/4} + c_3 e^{-\mathrm{i}\pi/4}\zeta^{5/4})\right)/\mu(\zeta) \quad z \in \Omega_3, \end{aligned} \tag{34}$$

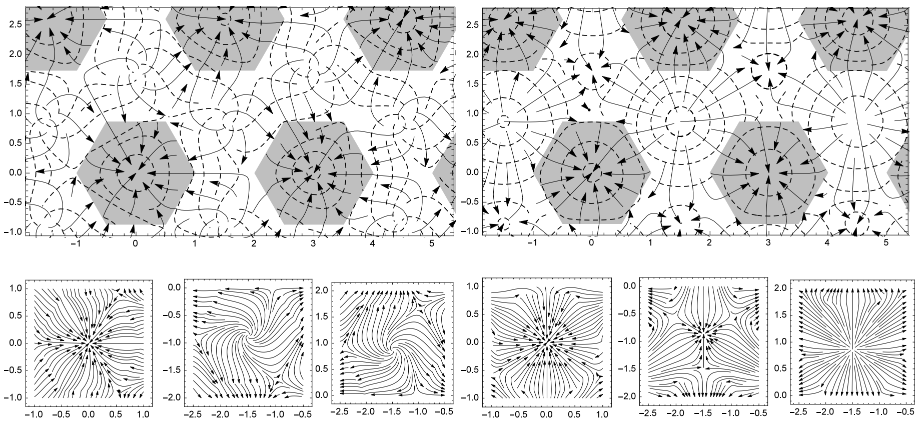

Figure 10: $\rho_1 = 1$, $\rho_2 = \rho_3 = 10$, $Q_2 = 1$, $Q_3 = 1$, $\Gamma_2 = 1$, $\Gamma_3 = -1$ (left panel), $\rho_1 = 1$, $\rho_2 = \rho_3 = 0.1$, $Q_2 = -1$, $Q_3 = 3$, $\Gamma_2 = 0$, $\Gamma_3 = 0$ (right panel)

For this case $Q_1 = \Gamma_1 = 0$ and the first solvability condition (27) gives $Q_2 = -Q_3$. The second condition (27) is fulfilled in the limit form, that is, $\rho_1\Gamma_1 \to -(\rho_2\Gamma_2 + \rho_3\Gamma_3)$ when $\rho_1 \to \infty$ and $\Gamma_1 \to 0$. If $Q_2 = -Q_3$, then real parameters c_j, defined from the conditions (4), are equal

$$c_1 = \frac{(\Gamma_2 - \Gamma_3)\mu_0}{4\pi}, \quad c_2 = \frac{(\Gamma_2 + \Gamma_3 + 2Q_2)\mu_0}{4\sqrt{2}\pi}, \quad c_3 = \frac{(\Gamma_2 + \Gamma_3 - 2Q_2)\mu_0}{4\sqrt{2}\pi}. \tag{35}$$

Summing up the latest results, we formulate the following statement.

Theorem 4. *If* $\rho_2 = \rho_3$, $\rho_1 < \infty$ ($\rho_1 = \infty$) *and the solvability conditions* (27) *are satisfied* ($Q_2 = -Q_3$) , *then the unique solution of the problem* (2), (4) *is defined by the formulae* (32), (33) ((34), (35)).

The distribution of streamlines and equipotentials, plotted in accordance with formulae (34), (35) is shown in the Fig. 11 for two sets of parameters.

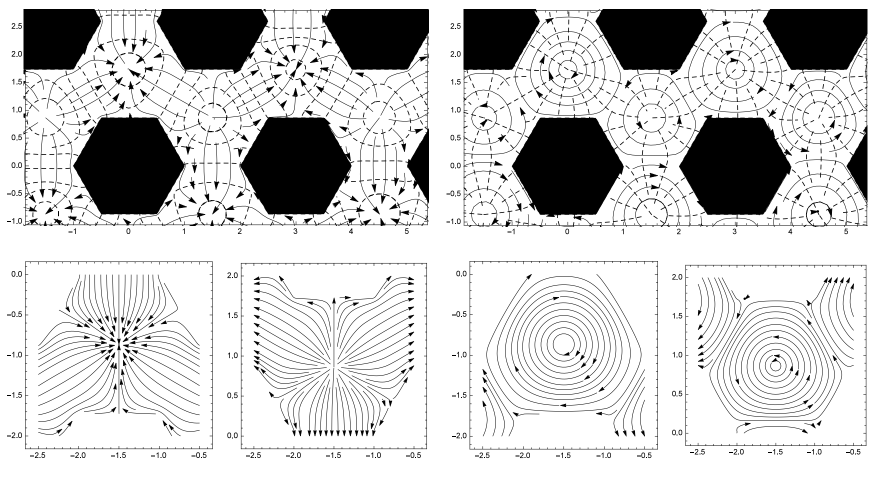

Figure 11: $\rho_1 = \infty$, $\rho_2 = \rho_3 = 5$, $Q_2 = -2$, $Q_3 = 2$, $\Gamma_2 = 0$, $\Gamma_3 = 0$ (left panel), $Q_2 = 0$, $Q_3 = 0$, $\Gamma_2 = -4$, $\Gamma_3 = 2$ (right panel)

At last, if $\rho_1 = \rho_2 = \rho_3$, that is, we have a homogeneous medium with a flow generated by three sets of doubly periodically distributed vortex–sinks/sourses. On this occasion $a =$

$b = c = 0$ and from the formulae (20) through (25) we obtain

$$v_1(z) = v_2(z) = v_3(z) = \frac{C_1 + C_2\zeta}{\mu(\zeta)}.$$

Here C_1, C_2 are arbitrary complex parameters that must be determined through the conditions (4). In accordance with (15) we obtain

$$\mu_0 \mathrm{res}_{O_k} v_k(z) = C_1 \varepsilon^{-2(k-1)} + C_2 \varepsilon^{2(k-1)} = \frac{\mu_0(Q_k - \mathrm{i}\Gamma_k)}{2\pi}, \quad k = 1, 2, 3.$$

Summing up the last three equations, we obtain the following necessary and sufficient solvability conditions:

$$Q_1 + Q_2 + Q_3 = 0, \qquad \Gamma_1 + \Gamma_2 + \Gamma_3 = 0,$$

which correlate with the assertions of Theorem 1. If these conditions are met, then our system has the unique solution

$$C_{1,2} = \pm \frac{\mathrm{i}\mu_0}{2\sqrt{3}\pi} \left[(Q_1 - \mathrm{i}\Gamma_1)\mathrm{e}^{\mp \mathrm{i}\pi/3} + (Q_2 - \mathrm{i}\Gamma_2) \right].$$

The distribution of flow nets in a homogeneous medium is shown in Fig. 12 for two special cases.

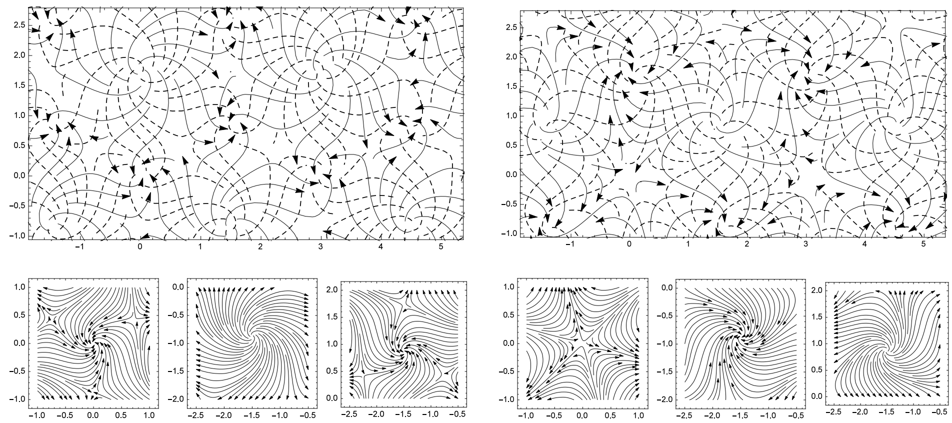

Figure 12: $\rho_1 = \rho_2 = \rho_3 = 1$, $Q_1 = -1$, $Q_2 = 2$, $\Gamma_1 = -1$, $\Gamma_2 = -1$ (left panel) $Q_1 = 0$, $Q_2 = -2$, $\Gamma_1 = 0$, $\Gamma_2 = -2$ (right panel)

4 Concluding remarks

The present work is a direct continuation of our previous results obtained for the four-phase rectangular ([2]) and three-phase diamond ([3]) checkerboards. The structure we consider here, has three distinct phases, and is composed of regular hexagons. Unlike all previously published works on doubly periodic n-phased structures, we considered a case with a flow generated not by a single dipole at infinity, but by three sets of identical in each phase vortex–sinks/sources. The same basic idea as in the above cited papers was used to find a solution for a hexagonal tessellation. That is, we again use conformal mappings to reduce a doubly periodic ℝ-linear conjugation problem to RH problem for three sectors posed on three-sheeted Riemann surface. It so fell out that the last problem has identical boundary conditions on all three sheets. Moreover, these conditions exactly coincided with the corresponding conditions in [3]. This made it possible to find a general solution to the original boundary value problem

(1), and then its specific solution that satisfies the additional conditions (4). The necessary and sufficient solvability conditions (27) obtained in the solution process are, from our point of view, of independent interest.

The following special cases are considered: the case when two of the three phases have the same resistivities; the case of one non-conducted phase; the case of homogeneous material. Explicit solutions are derived for all these cases. As such, these solutions are the first and only explicit ones for field in doubly-periodic heterogeneous structures generated by the corresponding sets of vortexes/sinks/sources.

It would be interesting to generalize the solved problem in the case of arbitrary locations of sinks and sources in each elementary cell. Also the case of a flow in a hexagonal checkerboard, generated by a single dipole at infinity, is our long-standing goal.

Acknowledgements

This work was supported by the subsidy allocated to Kazan Federal University for the state assignment in the sphere of scientific activities, project 1.12878.2018/12.1.

References

[1] V. L. Berdichevski, *The thermal conductivity of chess structures*, Vestn. Mosk. Univ. Mat. Mech., 40 (1985), pp. 56–63. (In Russian).

[2] R. V. Craster and Y. V. Obnosov, *Four phase periodic composites*, SIAM J. Appl. Math., 61 (2001), pp. 1839–1856.

[3] R. V. Craster and Y. V. Obnosov, *A three phase tessellation: solution and effective properties*, Proc. R. Soc. Lond. A., 460 (2004), pp. 1017–1037.

[4] Crowdy, D. G., *Analytical formulae for source and sink flows in multiply connected domains*, Theoretical and Computational Fluid Dynamics, 27 (1-2) (2013), pp. 1-19 DOI: 10.1007/s00162-012-0258-x

[5] Crowdy, D. G., *Uniform flow past a periodic array of cylinders*, European Journal of Mechanics, B/Fluids, 56, 1 March (2016), pp. 120-129.

[6] Drygas, P.,Gluzman, S., Mityushev, V. Nawalaniec, W., *Effective elastic constants of hexagonal array of soft fibers*, Computational Materials Science, 139, November (2017), pp. 395-405.

[7] Yu. P. Emets, *Electrical characteristics of composite materials with regular structure*, Kiev: Naukova Dumka,(1986) (in Russian)

[8] 74. Anatolii Kazarin, Yurii Obnosov, *An exact analytical solution of an R-linear conjugation problem for a n-phased concentric circular heterogeneous structure*. Appl. Math. Modell., 40(9-10) (2016), pp. 5292-5300. Doi: 10.1016/j.apm.2015.12.027

[9] D. F. Lawden, *Elliptic functions and applications*, Springer-Verlag, 1989.

[10] Milton G.W., *The theory of composites*, Cambridge University Press, 2002.

[11] Milton, G.W., *Approximating the effective tensor as a function of the component tensors in two-dimensional composites of two anisotropic phases*, SIAM Journal on Mathematical Analysis, 50(3), (2018), pp. 33273364.

[12] V.Mityushev, *Exact solution of the Rlinear problem for a disk in a class of doubly periodic functions*, Journal of Applied Functional Analysis,2(2) (2007), pp. 115–127.

[13] Mityushev, V., Rylko, N., Bryla, M., *Conductivity of two-dimensional composites with randomly distributed elliptical inclusions*, ZAMM Zeitschrift fur Angewandte Mathematik und Mechanik, 98 (4), (2018), pp. 554–568

[14] Y. V. Obnosov, *Exact solution of a boundary-value problem for a rectangular checkerboard field*, Proc. Roy. Soc. Lond. A, 452 (1996), pp. 2423–2442.

[15] Y. V. Obnosov, *Periodic heterogeneous structures: new explicit solutions and effective characeristics of refraction of an imposed field*, SIAM J. Appl. Math., 59 (1999), pp. 1267–1287.

[16] Y. V. Obnosov, *Generalized Milne-Thomson theorem*, Applied Mathematics Letters, 19 (2006), pp. 581-586. doi:10.1016/j.aml.2005.08.006

[17] Y. V. Obnosov, *Three-phase eccentric annulus subjected to a potential field induced by arbitrary singularities*, Quart. Appl. Math. 69 (2011), pp. 771-786. s0033-569x(2011)01242-8

[18] Obnosov Y. V., Fadeev A.V. , *A generalized Miln-Thomson theorem for the case of elliptical inclusion*, Euro Jnl of Applied Mathematics. 23 (4) (2012), pp. 469-484, Cambridge University Press . Doi:10.1017/S0956792512000058

[19] Y. V. Obnosov, *An R-linear conjugation problem for a plane two-component heterogeneous structure with an array of periodically distributed sinks/sources*, Appl. Math. Modell., 37 (2013), pp. 2830-2837, ttp://dx.doi.org/10.1016/j.apm.2012.06.028

[20] J. W. Rayleigh, *On the influence of obstacles arranged in rectangular order upon the properties of the medium*, Phil. Mag., 34 (1892), pp. 481–502.

[21] S. Wolfram, *Mathematica: A system for doing mathematics by computer*, Addison-Wesley, 1991.